Int. J. Electrochem. Sci., 11 **(2016)** 9088 – 9099, doi: 10.20964/2016.11.69

International Journal of ELECTROCHEMICAL SCIENCE
www.electrochemsci.org

Electrolyte Factors Influencing Separated Pore Growth of Anodic TiO_2 Nanotube Arrays

Sorachon Yoriya[*] *and Angkana Chumphu*

National Metal and Materials Technology Center, 114 Thailand Science Park, Pahonyothin Road, Khlong 1, Khlong Luang, PathumThani 12120, Thailand
[*]E-mail: sorachy@mtec.or.th

Received: 26 July 2016 / *Accepted:* 15 September 2016 / *Published:* 10 October 2016

This work presents an investigation of electrolyte properties in relation to the growth of TiO_2 nanotube array films, particularly concerning the measurement of conductivity in the diethylene glycol-hydrofluoric-water electrolyte system. The work aims to elucidate the behavior of ions in the anodized electrolytes with a better insight into the relation between molar conductivity and concentration of the additives. Differing solvation of the fluoride ion in various composition of water in the DEG-H_2O mixture is attributed to the major factor determining the capability of proton transfer, controlling the ionic mobilities and the molar conductivities. Applying the feature of the two-factorial experiment has demonstrated a clear interaction of electrolyte parameters and titanium concentration dissolving into the electrolyte, which is believed to be a combination effect on pore widening and separating of nanotubes. A proposed schematic drawing has been demonstrated, summarizing how the nanotube arrays are constructed as a consequence of varying electrolyte type and composition.

Keywords: TiO_2 nanotube arrays, electrochemical anodization, tube separation, electrolyte conductivity

1. INTRODUCTION

Fabrication of TiO_2 nanotube arrays has been extensively studied during the past years. A facile pathway to synthesize highly ordered, vertically oriented TiO_2 nanotubes arrays is electrochemical anodization. This technique offers unique morphological architectures, precisely controllable dimensions, and related remarkable properties of TiO_2 nanotubes arrays making them desirable for many applications. The anodic TiO_2 nanotube arrays have demonstrated their utility in dye-sensitized solar cells (DSSC),[1-2] high-performance hydrogen sensors, [3-4] water photoelectrolysis, [5]

biomedical devices such as drug delivery, [6-7] tissue engineering, [8-10] platforms for bone and scaffolds due to great biocompatibility, non-toxicity and environmental safety. [11-13]

Most of the previous work reported has focused on the use of electrolyte containing fluoride ion, considered as the promising choice of electrolyte for successfully producing the tubular structure of TiO_2 nanotubes arrays. Hydrofluoric acid and ammonium fluoride with proper concentration per each morphological need was found to be crucial for the formation of nanotubes. The flexibility of the anodization process has shown its great ability to grow TiO_2 nanotubes with different morphologies and pore arrangement. The advance in the anodic fabrication has made it possible to prepare the extremely unique nanotube dimensions with controllable properties suitably potential for their applications. For example, the large pore diameter 400-900 nm with optical wavelength-sized apertures, [14-15] the long tube length up to 1000 μm, the largest to date, for use as functional filtration membrane, [16] and controllable wall thickness of 7-34 nm for great performance in electronic devices and heterojunction cells. [12, 17] Further, the 20 nm pore diameter of titania nanotubes has been achieved for improved bladder stent. [18] Many rapid synthesis of TiO_2 nanotube arrays in few minutes to achieve high aspect ratio have been reported mostly using ethylene glycol electrolyte. [19] The formation of TiO_2 nanotubes arrays is a direct consequence of proper optimization among the important parameters involving the anodic film fabrication.

In the electrolyte containing fluoride ions, dissolution of TiO_2 ($TiO_2+4H^+ + 6F^- \rightarrow [TiF_6^{2-}] + 2H_2O$) leads to the formation of titanium-hexafluoro complex, which is well dissolved and stable in electrolyte.[20] The electrochemical dissolution of titanium oxides generates the oxygen anion species (OH^- and O^{2-}) and results in the injection of O^{2-} into the oxide layer. At steady state, the amount of O^{2-} generated at the oxide surface is equal to the flux of oxygen ions at the oxide/electrolyte interface. The large fraction of titanium is transformed into the soluble species in electrolyte that subsequently affects the electrolyte properties due to the dissolution process, with only ~ 2 % of Ti converting into nanotube and the barrier oxide layer. [21] Loss of titanium was expected to play a significant role in generating the film porosity. [22-23] As far as the formation mechanism of anodic titania nanotubes is concerned, the electrochemical behavior of the oxide/electrolyte interface and physical properties of the oxide films are considered of great interest to promote progress in field of modeling nanochannel oxide growth. The formation of an oxide layer on the metal substrate has been studied particularly in recent years, various anodic concepts and theoretical models have been postulated to explain the growth of the self-organized titania nanotubes, for example, localized dissolution model, [5, 24-29] high field model that the film growth rate is limited by migration of ionic species (e.g. Ti^{4+} and O^{2-}) through the oxide film [30-33] The oxide composition change may occur from the addition of O^{2-} into the oxide where OH^- is acidified at the oxide/electrolyte interface: $OH^-_{aq} \rightleftharpoons O^{2-}_{OX} + H^+_{aq}$. The equifield strength model has been proposed to explain the dependence of pore formation and separation of nanotubes. [34] Self organization of nanopores is mainly governed by electric field facilitating the electrochemical reactions at the metal/oxide and oxide/electrolyte interfaces, when the oxidation and dissolution rates of the oxide are in equilibrium. The nanotube separation has been considered as a result of Ti^{4+} dissolution into electrolyte generating cation vacancies based on the point defect model. [29] Nonetheless, the mechanistic view of nanopore array formation on a particular aspect of physical properties of electrolyte corresponding structure is considerably less reported and still not fully

understood.

In this work, we present the study of electrochemical anodization in diethylene glycol (DEG)-based electrolyte, particularly focusing on the investigation of electrolyte properties in various concentrations and types of the additive component incorporating into the DEG solvent. Conductivity of electrolyte is a result of the transport of ions. In this study, conductivity parameter changing with the composition has been examined to understand its role on the growth of nanotubes. The relation of molar conductivity and concentration is further to be carried out to evaluate the behavior of ions in the electrolyte. Tendency of the nanotube growth with pore widening and larger tube separation as depending upon hydrofluoric acid and water is to be presented, with the effect of fluoride ion solvation and proton transfer ability also to be described.

2. EXPERIMENTAL

Titanium foils (0.25 mm, 99.7%; Sigma-Aldrich) were cleaned with acetone and iso-propanol prior to anodization. Herein anodization were performed potentiostatically using two-electrode electrochemical cell at the controlled temperature bath of 20±3 °C, a rectangular platinum foil as cathode. The interelectrode spacing was kept at 2.0 cm to remain consistency of the result.[Ref-Oh] Anodizing electrolytes were prepared in a combination of diethylene glycol (DEG, 99.7%, Sigma-Aldrich), hydrofluoric acid (HF, 48% aq. Solution, Merck), and de-ionized water, with the electrolyte composition designed to systematically vary to obtain the surface plot of conditions. The electrolyte conditions prepared in this study are as follows: DEG-2%HF-3%H_2O, DEG-2%HF-5%H_2O, DEG-4%HF-3%H_2O, and DEG-4%HF-5%H_2O, with these electrolytes subject to anodization voltage at 60 V and duration for 24 and 48 h. The soaked area of Ti in the electrolyte was held fixed approximately at 3.0 cm^2. The electrolytes after anodization were characterized their properties in comparison to the electrolyte prior to anodization. Titanium concentration in the anodized electrolyte was examined by inductively coupled plasma atomic emission spectrometry (ICP-AES, Perfin-Elmer Optima 5300 ICP). Conductivity was measured using conductivity meter (Eutech instrument Cyber Scan PCD650) Morphological study of the TiO_2 nanotube arrays was characterized by scanning electron microscope (FE-SEM, Leo 1530) and (Zeiss Supra 40)

3. RESULT AND DISCUSSION

Morphology of the TiO_2 nanotube array films has been studied. Figure 1 show FESEM images of the nanotube arrays anodized in various composition of electrolyte. Increasing water content in the electrolyte yielded the nanotube arrays with the relatively larger pore diameter. The average pore size and tube length of the nanotubes grown in different conditions are shown in Table 1.

Pore size seemed to reach its limit at about 250 nm. The dissolution of nanotube wall limits the achieved nanotube length. On further increasing water content up to 9%, the window range of pore diameter was pushed forward up to 300 nm, for a given applied voltage of 60 V and 24 h anodization

duration; see the top view image of the DEG-2%HF-9%H_2O in Figure 6. While using 5% water content for the DEG-4%HF, it was found that the nanotubes were not well-defined; the tubular structure could not survive to be observed after 24 h period. The anodization current density for the variation of water has been reported in the previous work. [35]

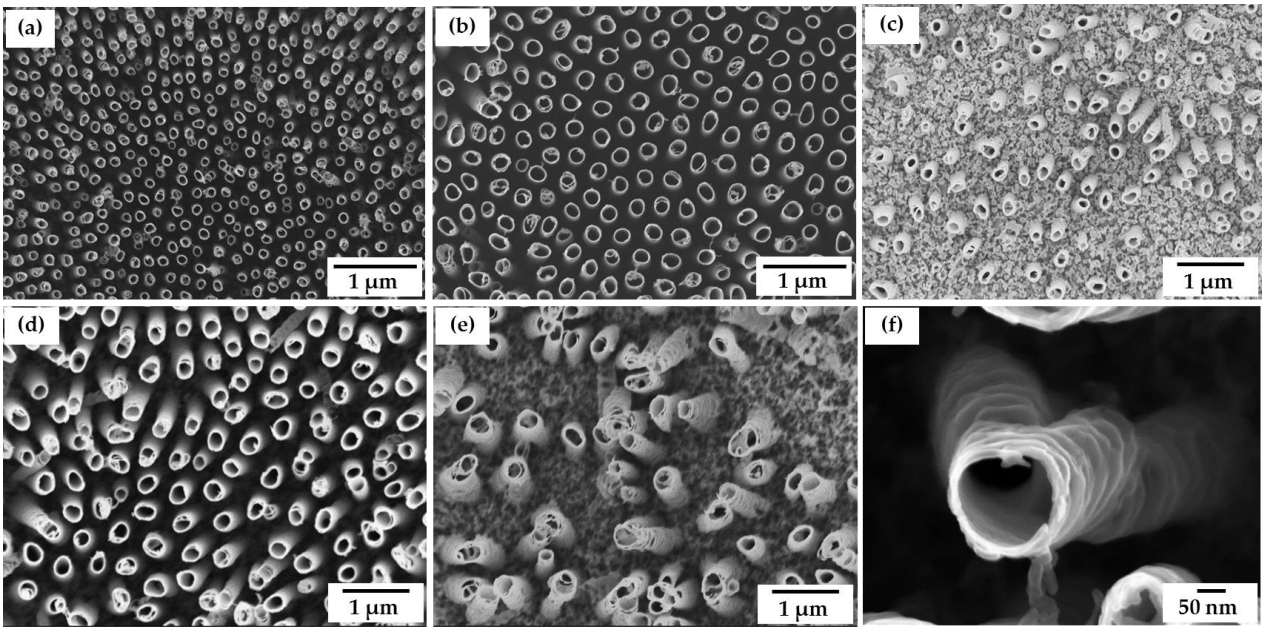

Figure 1. FESEM images of TiO_2 nanotube array films anodized in (a) DEG-2%HF-3%H_2O (24 h), (b) DEG-2%HF-5%H_2O (24 h), (c) DEG-4%HF-3%H_2O (24 h), (d) DEG-2%HF-3%H_2O (48 h), and (e) DEG-2%HF-5%H_2O (48 h). All the array films in (a)-(e) were performed under a fixed 60 V. The TiO_2 nanotube was magnified at high magnification showing tube splitting under a pore (f); the film was grown in the same condition as figure (a).

Table 1. Average pore diameter and tube length of TiO_2 nanotube arrays obtained from different electrolyte composition.

Condition	Average pore diameter (nm)	Average tube length (μm)
DEG-2%HF-3%H_2O, 24 h	130	2.0
DEG-2%HF-3%H_2O, 48 h	230	2.5
DEG-2%HF-5%H_2O, 24 h	220	1.0
DEG-2%HF-5%H_2O, 48 h	250	1.3
DEG-4%HF-3%H_2O, 24 h	150	0.7

It is noteworthy to mention the influence of fluoride concentration on the nanotube growth with large tube-to-tube spacing. Increasing HF content, a slight increase in pore diameter was obtained; 130 nm for 2% and 150 nm for 4%. Apparently with more acid addition, there is small difference in pore diameter, but obviously significant in tube separation. It is well evidence that the tubes stand separately and locate randomly on the anodic surface. The influence of anodization time (48 h) for Figure 1 (d)

and (e) has shown the result on pore widening and pore separation with increasing water content; the average pore size of the conditions (d) and (e) is 230 nm and 250 nm. The effect of water is more pronounced for the condition of Figure 1 (e), which is DEG-2%HF-5%H_2O (48 h). The chemical dissolution of TiO_2 becomes predominant governing the process at prolonged anodization period, [12, 14] resulting in considerably etching on the nanotube wall reflecting such spring-like evidence of the tube surface.

In addition, pore splitting of nanotubes could be observed for the DEG-HF-H_2O system as shown in Figure 1 (f). Because of the presence of F^- ions, dissolution of the oxide barrier occurs randomly on the surface, forming small pits. Then the tube formation is determined by the pit formation or the growth of pits into pores, while the pore initiation occurs at randomly distributed sites leading to an organized array. Propagation of small pits eventually results in the larger pores. [12] For this case, the tube branching mechanism is presumed to dominate the populating process, possibly occurring due to the use of high HF and water concentration. [36] The tube density can be related to the anodization and the times of branching of the initial nanotubes, which can be calculated as depending upon density and molar mass of TiO_2, current transient, and average tube length of nanotubes between each branching.

Figure 2 shows the increase in titanium concentration as a function of HF and water content in the electrolyte. The overlay of the surface plot is clearly illustrated. In this study, titanium concentration was investigated to confirm its result as a direct consequence of the varied electrolyte parameters. The window range of electrolyte has been designed by applying an important feature of the two-factorial experiment to this study in order to obtain a clear view of surface plot of experiment data, possibly achieving the interaction of parameters. The designed experiment has indicated a clear evidence that electrolyte composition has shown its combination effect on the increased Ti concentration. As increasing HF concentration, titanium was found to dissolve into the anodized electrolyte in the higher amount with respect to the increase in water content. This could be explained by the more diffusion and high mobility of fluoride ions moving towards the titanium surface and hence leading to the more extraction of titanium into the electrolyte. With prolonged anodization time, the effect of higher HF concentration is more predominant, obviously revealing the more increase in titanium concentration in the electrolytes.

Considering the oxide/electrolyte interface, the Ti^{4+} dissolving into electrolyte generating cation vacancies can be expressed as $Ti_{Ti}(ox) \rightarrow Ti^{4+}(aq) + V_{Ti}^{4-}(ox)$, [29] where $Ti_{Ti}(ox)$ is titanium atom in titanium lattice position in the oxide layer, $Ti^{4+}(aq)$ is titanium cation dissolving in electrolyte, and $V_{Ti}^{4-}(ox)$ is cation vacancy in the oxide lattice, based on the point defect model. When the generation of titanium cation vacancies and oxygen vacancies is unbalanced, the void condensation could lead to the separation of walls. In the case of fast oxide dissolution rate, e.g. in which the electrolyte containing high HF content, the faster generation of cation vacancies occurs at the outer wall layer, the density of cation vacancies is higher especially in acidified fluoride solution. The cation vacancies transport radially leading to the enhanced repulsive forces between walls and consequently the pore separation. Pore separation forming individual nanotubes can also occur under the proper electrochemical conditions at high anodization current. [37] The combination effect of titanium

dissolution improving the electrolyte conductivity over the anodization period is believed to be the key factor influencing the nanotube separation.

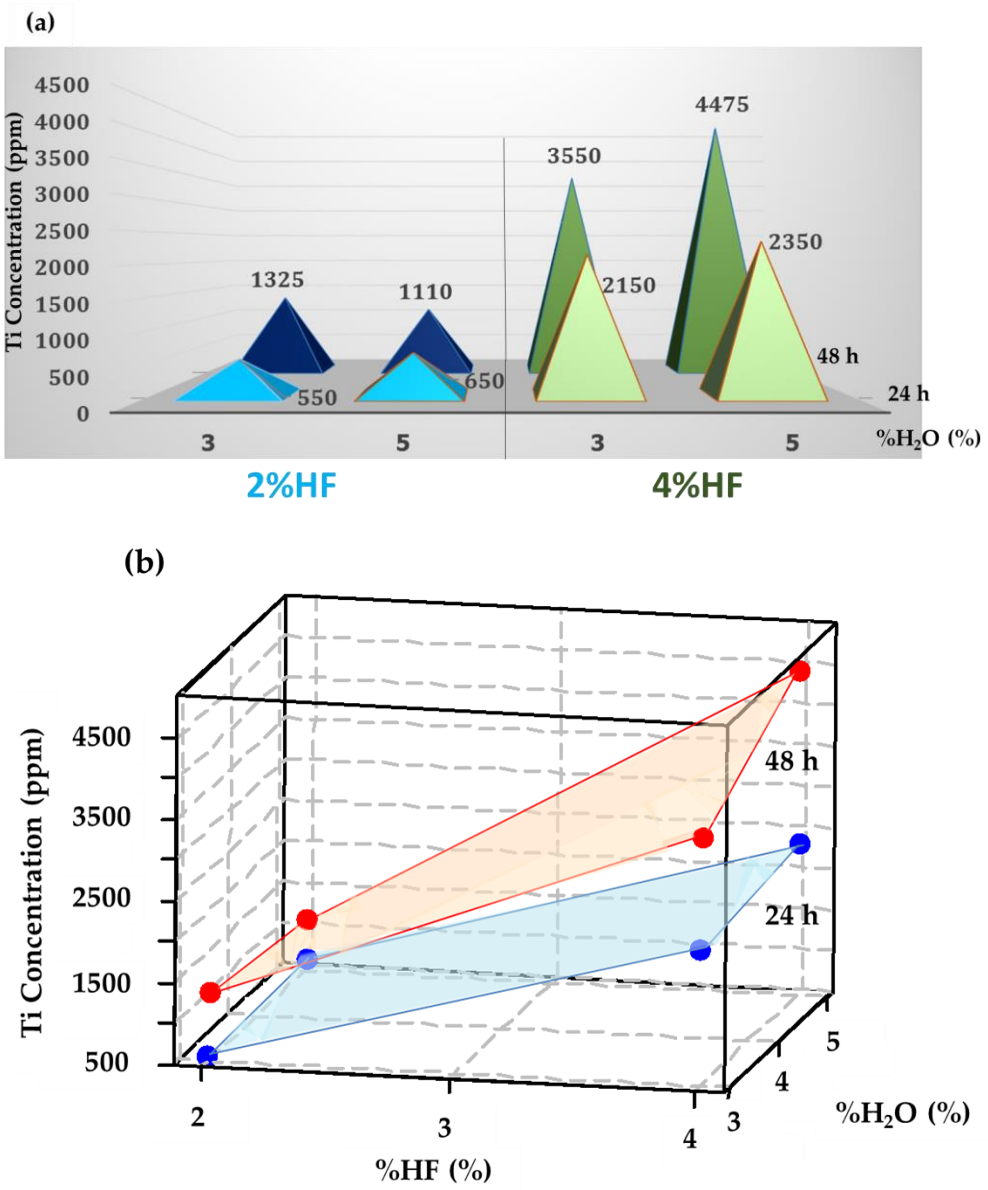

Figure 2. (a) Column demonstration of Ti concentration measured from the anodized DEG-HF-H_2O electrolytes at various contents of HF and H_2O, as the anodization time was fixed for 24 h and 48 h. (b) An overlay surface plot of Ti concentration for the conditions mentioned in Figure (a).

Conductivity, a result of the transport of ions, was measured to obtain the analytical and physicochemical information. In this study, the increase in electrolyte conductivity was well confirmed that is strongly due to the increase in titanium concentration. The conductivity of non-aqueous electrolyte, described by the well-known Debye-Huckel-Onsager limiting law, depends on electrolyte concentration, ionic charges, viscosity, and relative permittivity. A similar form of relation has been theoretically obtained by Kohlrausch's law, the law of independent migration of ion for dilute solutions: $\Lambda = \Lambda^{\infty} - kc^{1/2}$, where k is a constant, and molar conductivity, Λ (S cm^2 mol^{-1}), of each

condition can be determined in relation to its concentration *c*. Whereas the Λ^{∞} is limiting molar conductivity that can confirm the complete dissociation of the electrolyte. [38] Herein, the molar conductivity of anodized electrolyte has been investigated by applying the Kohlrausch's law to explore the behavior of molar conductivity in various compositions of electrolytes. The values of Λ and $c^{1/2}$ were determined and plotted in Figure 3. The Λ value of the DEG electrolytes containing HF decreases linearly with the increase in $c^{1/2}$, confirming that the increase in HF concentration leading to the increase in ionic conductivity. From such linear behavior, the curve agrees well with the Kohlrausch's equation where the effect of short-range ionic interaction has not taken into account. This theory is applicable to predict the behavior of ions in the DEG-HF electrolyte system, particularly containing small amount of water, from the experimental $\Lambda - c^{1/2}$ relation. From the plot, we could obtain the approximate value of Λ^{∞} and *k* from the extrapolation and the slope respectively: 1.3554 S cm^2 mol^{-1} and 0.1744, for the anodized electrolyte mixture containing a variation of ionic species.

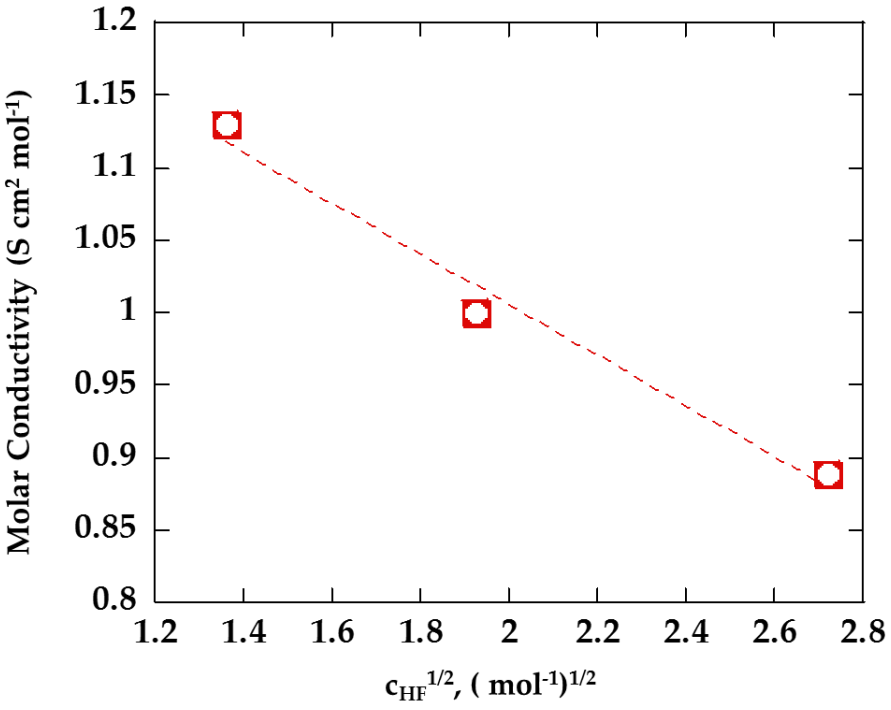

Figure 3. A plot of Λ against $c^{1/2}$ determined for the DEG-HF electrolyte conditions using different HF concentrations: 0.135, 0.27, and 0.54 M

The effect of increasing HF content in electrolyte contributes the numerically higher conductivity than the effect of increasing water content as the plot shown in Figure 4. Varying water content in the electrolyte was found to yield the nonlinear curve over the variation range of water. Particularly at the high water contents, no substantial change of Λ was observed; the Λ values lie in the close range of 0.43-0.44 S cm^2 mol^{-1}. More water addition did not show significant change in molar conductivity. This could be ascribed to the competition between the increase in the charge carrier number and the decrease in ionic mobilities, as the ion-ion interactions of different size of ions becoming stronger. In such a case, either solvation– ion association occurring by forming ionic atmosphere, or solvent relaxation– moving ion subjected to a retarding force due to the atmosphere, is

believed to play a key role in determining the ionic mobilities and the molar conductivities. [39-40] For the curve in Figure 4, the Λ^{∞} could be obtained from extrapolation, as many developed theories from the Debye-Huckel-Onsager theory have been proposed for a better yield of limiting molar conductivity, by taking into account both the long-range and short-range ionic interactions, ionic charges, and solvent properties. For example, the Fuoss-Hsia equation has been proposed to explain the behavior of ions in different degree of association region. [38]

Considering the increase in acidity for pore initiation with the increased HF concentration, one may be discussed in terms of proton transfer ability. In dilute aqueous solution, an isolated HF molecule donates a proton to an aggregate of water molecules forming an aquated fluoride ion (HF_2^-), which occurs in the symmetrical anion form. [41] Considering the mixture of HF-H_2O in DEG system, the dissociation of HF in water is complicated as both proton and fluoride ions are solvated and form the stable species as follows: $3HF \rightleftharpoons H_2F^+ + HF_2^-$. As a solute in DEG-$H_2O$, HF is a fairly weak acid. When only a small amount of water is present in the system, a proton from polymeric hydrogen fluoride is transferred to an isolated water molecule, and the fluoride ion is part of a stable polymeric anionic complex. As the HF concentration increases in the HF-H_2O mixtures, the system becomes progressively more acidic. On further increase in water composition, the larger amount of water could allow the more degree of molecular interactions, differing solvation of the fluoride ion in the DEG-H_2O mixture. Such various scale of solvation of acid/water molecules is attributed to the considerably more attention factor determining the capability of proton transfer.

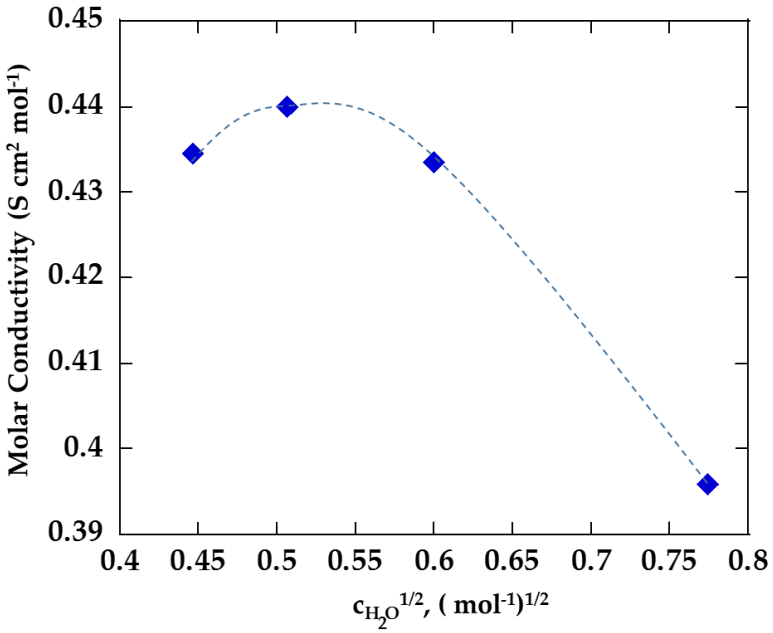

Figure 4. A plot of Λ against $c^{1/2}$ determined for the DEG-2%HF electrolyte containing different water contents; 3, 5, 7, 9%.

In addition, the conductivity is determined by solvent viscosity and ionic radii. [38] Varying water content, the increase in conductivity in relation to the decrease in viscosity is shown in Figure 5. The Stokes' radii of ions dissociating in the electrolytes could possibly vary from condition to another, thus reflecting the variation in ion solvation. In the electrochemical process, migration of ions such as

metal ion, oxygen anions, or fluoride ions in electrolyte is a key role in governing the formation of anodic TiO_2 and controlling the tube morphology. [42-43] The ionic radius of ions directly affects the migration rates in electrolyte; the larger ionic size is the slower migration rate. For example, the migration rate of the smaller ionic radius of F^- (0.119 nm) is faster than that of the larger size of O^{2-} ion (0.126 nm). [44] The fluoride ion migrates inward at twice the rate of O^{2-} ions, hence developing the fluoride composition in the oxide layer. The penetration depth of migrating F^- ions is determined by the migration rate of F^- and transport number in relation to those values of O^{2-} under the applied field. The transport number of Ti^{4+} and O^{2-} in the titania film is 0.39± 0.03 [43] and 0.6. [45] To some extent, the incorporation of fluoride ions in the anodic film gives rise to the film detachment from the metal substrate leading to the poor film properties to be obtained. [44] In other words, the TiO_2 film detachment is because of the formation of titanium fluoride layer occurring at the metal/oxide interface that results from the fast inward migration of F^- through the oxide film during anodization under the high electric field. Thus, to this point of view, solvation effect on fluoride ion is considerably important. In the viscous electrolyte at low temperature, the chemical etching of TiO_2 by F^- was found to be very low, as only small difference in pore diameter was normally obtained. [46] Nonetheless, the pore pitting and etching rates are needed to be tailored by selecting a proper electrolyte medium with a well manipulation of electrolyte composition.

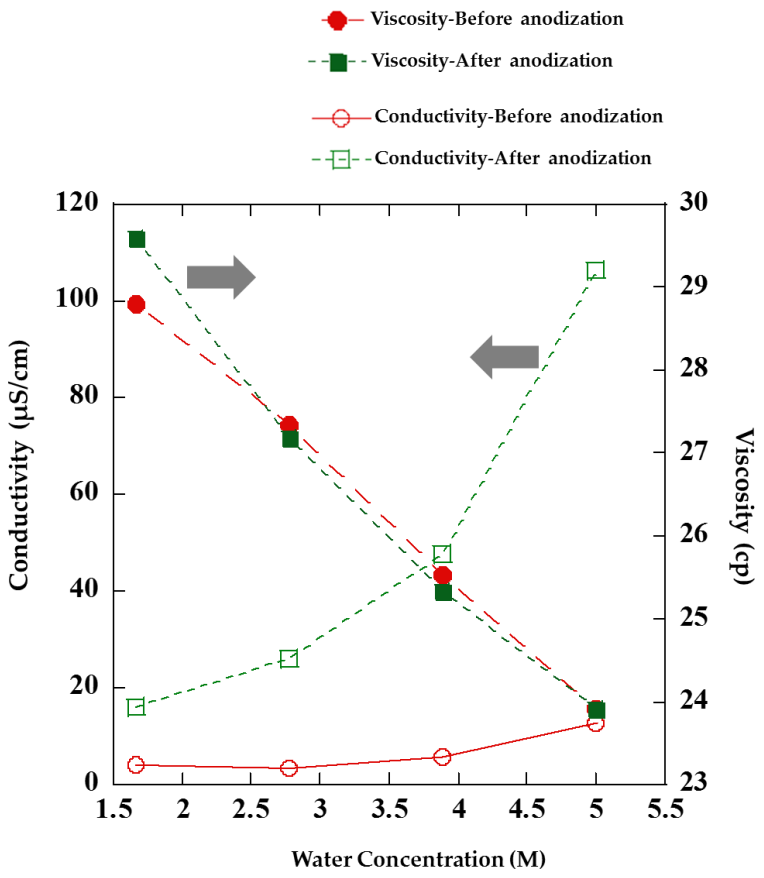

Figure 5. Conductivity and viscosity of the DEG-HF-*x*%H_2O electrolytes plotted as a function of water concentration. The electrolytes both before and after anodization were measured in comparison. The varied water contents of 3, 5, 7, 9% are shown in 1.67, 2.78, 3.89, 5.00 M, respectively.

Figure 6 summarized the electrolyte parameters influencing the nanotube morphology and pore arrangement through the schematic drawing proposed for the anodic titania nanotube arrays. It could be confirmed by the experimental result in this work that water content has a strong effect controlling the pore diameter of nanotubes, while HF content plays a key role determining the architectural orientation or the separation of nanotubes. A stronger electrolyte with more ion dissociation could possibly lead to the larger degrees of pore widening and more tube separating. The anodization time is considered to be a dominant fabrication process parameter that could shift the tendency of tube separation to the larger range. However, tailoring the electrolyte parameters is essentially needed for the complicated non-aqueous electrolyte mixture in order to remain the tubular structure with desire morphological dimensions on the anodic surface.

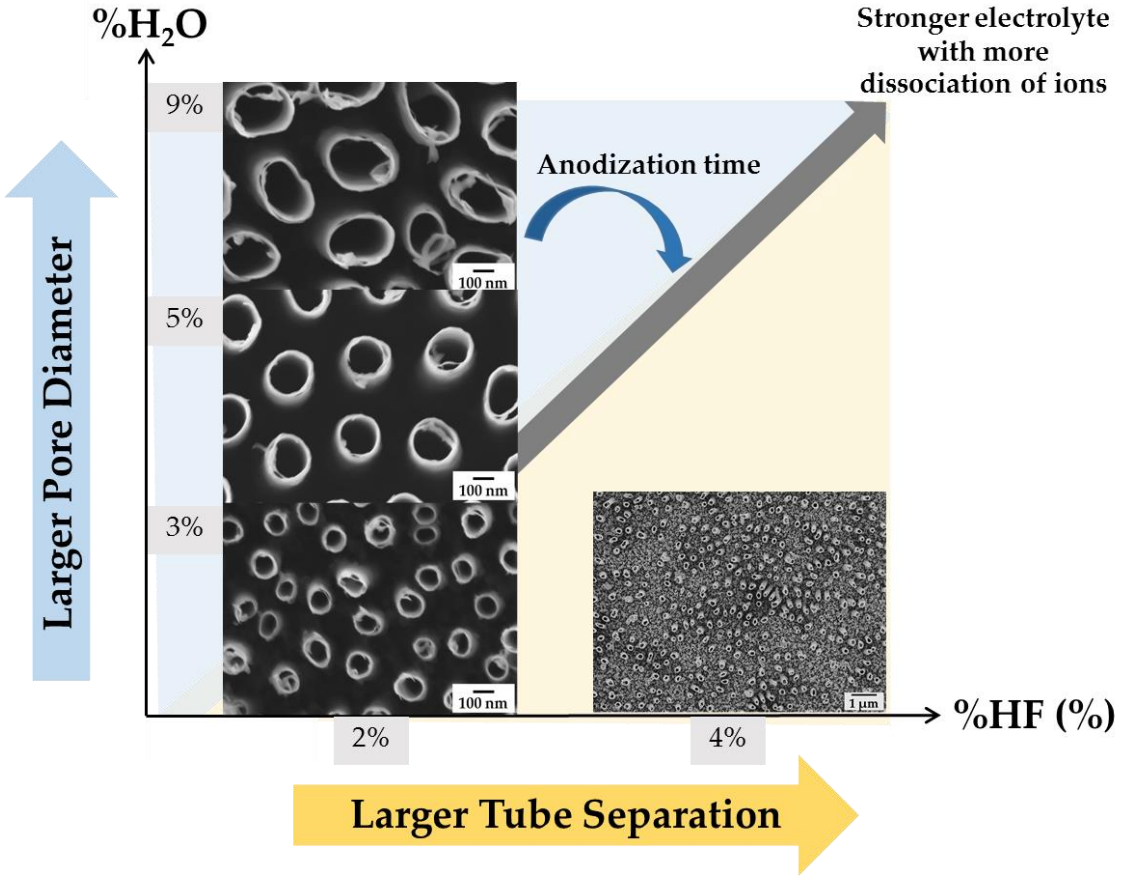

Figure 6. A proposed schematic illustration showing the influence of electrolyte composition on orientation and morphology of the anodic TiO_2 nanotubes.

4. CONCLUSION

This work reported a study of conductivity of the diethylene-based electrolytes after their use in the fabrication of TiO_2 nanotube array films. Applying the Kohlrausch's law to explore the behavior of molar conductivity in various composition. The result showed that the $\Lambda - c^{1/2}$ relation of the DEG-HF-H_2O system agrees well with the theory for the use of 3% water content; the limiting molar conductivity determined for this system is an approximate value of 1.3554 S cm^2 mol^{-1}. Different

degrees of solvation of fluoride ion in H_2O is attributed to the major factor determining the proton transfer ability, reflecting difference in ionic mobilities. Titanium concentration was investigated to confirm its strong effect on the increase conductivity of the anodized electrolytes. A stronger electrolyte with more ion dissociation could possibly lead to the larger degrees of pore widening and more tube separating, as a consequence of the use of high water and HF concentration. Important aspects in terms of mechanistic solvation and proton transfer ability has been described.

ACKNOWLEDGEMENTS
The authors acknowledge the National Metal and Materials Technology Center (MTEC), Thailand, for instrument facilities and providing research funding Grant no. P1100228 through the Ceramics Technology Research Unit. We are grateful to our international collaboration at BAM Federal Institue for Materials Research and Testing, Germany, for high resolution FESEM.

References

1. G. K. Mor, K. Shankar, M. Paulose, O. K. Varghese, and Craig A. Grimes, *Appl. Phys. Lett.91* (2007) 152111.
2. D. Kuang, J. r. m. Brillet, P. Chen, M. Takata, S. Uchida, H. Miura, K. Sumioka, S. M. Zakeeruddin, and M. Grätzel, *ACS Nano 2* (2008) 1113.
3. O. K. Varghese, D. Gong., M. Paulose, K. G. Ong, and C. A. Grimes, *Sens. Actuator B 93* (2003) 338.
4. M. Paulose, O. K. Varghese, G. K. Mor, C. A. Grimes, and K. G. Ong, *Nanotechnol.* 17 (2006) 398.
5. Gopal K. Mor, O. K. V., Maggie Paulose, Karthik Shankar and Craig A. Grimes *Sol. Energ. Mat. Sol.* 90 (2006) 2011.
6. L. Peng, A. D. Mendelsohn, T. J. LaTempa, S. Yoriya, C. A. Grimes, and T. A. Desai *Nano Lett.*9 (2009) 1932.
7. E. Gultepe E, D. Nagesha, S. Sridhar, M. Amiji, *Adv. Drug Deliv. Rev.* 62 (2010) 305.
8. K. C. Popat, E. E. L. Swan, V. Mukhatyara, K.-I. Chatvanichkula, G. K. Mor, C. A. Grimes, T. A. Desai, *Biomaterial 26* (2005) 4516.
9. T. Dey, P. Roy, B. Fabry, and P. Schmuki, *Acta Materialia* 7 (2011) 1873.
10. A.-M. Azad, R. Hershey, A. Aboelzahab, and V. Goel *Adv. Ortho.* ID 571652 (2011) 1.
11. K. C. Popat, K. I. Chatvanichkul, G. L. Barnes, T. J. Latempa, C. A. Grimes, and T. A. Desai, *J. Biomed. Mat. Res. A*, 80 A (2007) 955.
12. S. Rani, S. C. Roy, M. Paulose, O. K. Varghese, G. K. Mor, S. Kim, S. Yoriya, T. J. LaTempa, and C. A. Grimes, *Phys. Chem. Chem. Phys.* 12 (2010) 2780.
13. M. Kulkarni, A. Mazare, E. Gongadze, S. Perutkova, V. K-Iglic, I. Milosev, P. Schmuki, A. Iglic, and M. Mozetic *Nanotechnol.* 26 (2015) 062002.
14. S. Yoriya and C. A. Grimes *Langmuir* 26 (2010) 417
15. A. Mohammadpour and K. Shankar, *J. Mats. Chem.* 20 (2010) 8474.
16. Maggie Paulose, H. E. P., Oomman K. Varghese, Lily Peng, Ketul C. Popat, Gopal K. Mor, Tejal A. Desai, and Craig A. Grimes *The Journal of Physical Chemistry C* 111 (2007) 14992.
17. M. Paulose, K. Shankar, O. K. Varghese, G. K. Mor, and C. A. Grimes, *J. Phys. D-Appl. Phys.* 39 (2006) 2498.
18. E. Alpaslan, B. Ercan, and T. J. Webster *Inter. J. Nanomed.* 6 (2011), 219.
19. X-L. Sui, Z-B. Wang, Y-F. Xia, M. Yang, L. Zhao and D-M. Gu, *RSC Adv.* 5 (2015) 35518.
20. F. M. B. Hassan, H. Nanjo, H. Tetsuka, M. Kanakuubo, T. Aizawa, M. Nishioka, and T. Ebina, *Transactions* 16 (2009) 35.

21. W.-J. Lee, M. Alhoshan, and W. H. Smyrl, *J. Electrochem. Soc.* 153 (2006) B499.
22. G. E. Thompson, *Thin Solid Films* 297 (1997) 192.
23. A. Valota, D. J. LeClere, T. Hashimoto, P. Skeldon, G. E. Thompson, S. Berger, J. Kunze, and P. Schmuki, *Nanotechnol.* 19 (2008) 355701.
24. H. E. Prakasam, K. Shankar, M. Paulose, O. K. Varghese, C. A. Grimes, *J. Phys. Chem. C* 111 (2007) 7235.
25. G. K. Mor, O. K. Varghese, M. Paulose, N. Mukherjee, and C. A. Grimes, *J. Mat. Res.* 18 (2003) 2588.
26. V. P. Parkhutik and V. I. Shershulsky, *J. Phys. D: Appl. Phys.* 25, (1992) 1258.
27. G. E. Thompson, *Thin Sol. Films* 297 (1997), 192.
28. J. Siejka and C. Ortega, *J. Electrochem. Soc. Sol. Stat. Sci. Tech.* 124 (1977) 883.
29. D. D. Macdonald, *J. Electrochem. Soc.* 140, (1993) L27.
30. T. Ohtsuka, M. Masuda, and N. Sato, *J. Electrochem. Soc*. 132 (1985) 787.
31. G. E. Thompson, G. C. Wood, *Nature* 290 (1981) 230.
32. J. P. S. Pringle, *Electrochim. Acta* 25 (198) 1403.
33. J. W. Diggle, T. C. Downie, and C. W. Goulding, *Chem. Rev.* 69 (1969) 365.
34. Z. Su and W. Zhou, *Adv. Mater.* 20 (2008) 3663.
35. S. Yoriya and C. A. Grimes, *J. Mater. Chem.* 21 (2011) 102.
36. Y. Chen, H.-H. Lu, X.-M. Wang, and S.-S. Lu, *J. Mater. Chem.* 22 (2012) 5921.
37. K. S. Raja, M. Misra, K. Paramguru, *Electrochim. Acta* 51 (2005) 154.
38. Izutsu, K., *Electrochemistry in Nonaqueous Solutions* 2002, Wiley-VCH, New York.
39. S. Yoriya and N. Bao, *Int. J. Electrochem. Sci*. 9 (2014) 7182.
40. J. Barthel, R. Wachter, G. Schmeer, and H. Hilbinger, *J. Solution Chem.* 15 (1986) 531.
41. T. A. O'Donnel, *The Chemistry of Fluorine- Comprehensive Inorganic Chemistry*, Elsevier, 1973.
42. D. Gong, C. A. Grimes, O. K. Varghese, W. C. Hu, R. S. Singh, Z. Chen, E. C. Dickey, *J. Mat. Res.*16 (2001) 3331.
43. C. A. Grimes and G. K. Mor, *TiO_2 Nanotube Arrays: Synthesis, Properties, and Applications* 2009, Springer, New York.
44. H. Habazaki, K. Fushimi, K. Shimizu, P. Skeldon, and G. E. Thompson, *Electrochem. Comm.* 9 (2007) 1222.
45. G. C. Wood, P. Skeldon, G. E. Thompson, and K. Shimizu, *J. Electrochem. Soc.* 143 (1996) 74.
46. J. Wang and Z.Lin, *J. Phys. Chem. C* 113 (2009) 4026.